Fabrication and Operation of Flow-Through Tubular SOFCs for Electric Power and Synthesis Gas Cogeneration from Methane

Huangang Shi, Chao Su, Guangming Yang, and Ran Ran
State Key Laboratory of Materials-Oriented Chemical Engineering, College of Chemistry and Chemical Engineering, Nanjing University of Technology, No. 5 Xin Mofan Road, Nanjing 210009, China

Yong Hao
Institute of Engineering Thermophysics, Chinese Academy of Science, Beijing 100190, China

Moses O. Tade and Zongping Shao
Dept. of Chemical Engineering, Curtin University, Perth, Western Australia 6845, Australia

DOI 10.1002/aic.14312
Published online December 20, 2013 in Wiley Online Library (wileyonlinelibrary.com)

Flow-through type tubular solid oxide fuel cells were successfully fabricated and operated with a single-chamber configuration for realizing the simultaneous generation of electric power and synthesis gas from methane by integrating a downstream catalyst into the fuel cell reactor. A new operation mode, which completely eliminated the gas diffusion between cathode side and anode side, is proposed. The cell showed high open-circuit voltages of 1.02–1.08 V at the furnace temperature range of 650–800°C when operating on CH_4-O_2 gas mixture at a molar ratio of 2:1. A peak power density of approximately 300 mW cm^{-2} and a maximum power output of 1.5 W were achieved for a single cell with an effective cathode geometric surface area of 5.4 cm^2 at the furnace temperature of 750°C. The in-situ initialization of the cell using CH_4-O_2 gas mixture was also realized via applying an effective catalyst into the tubular cell. © 2013 American Institute of Chemical Engineers *AIChE J*, 60: 1036–1044, 2014
Keywords: solid oxide fuel cells, single chamber, methane, tubular cell, electric power

Introduction

As a type of electrochemical energy conversion devices, solid oxide fuel cells (SOFCs) have received considerable attention from academic, industry, public, and also governments during the past decades because of their high energy conversion efficiency and low emissions.[1–5] A typical single SOFC is composed of a porous anode, a porous cathode, and a dense electrolyte sandwiching them. The electrolyte separates the SOFC into anode and cathode chambers, and allows only a specific ion (e.g., H^+ or O^{2-}) to transport. For a general SOFC operating process, molecular oxygen is first adsorbed over the cathode surface, where it is reduced to O^{2-} by consuming four electrons from external circuit through a series of intermediate reaction steps, and then O^{2-} diffuses through the dense electrolyte to the anode side, where it reacts with fuel to release electrons, finally the electrons releasing from the anode transport through the external circuit to the cathode side to form a complete electric circuit. SOFCs are usually operated at elevated temperatures between 500 and 1000°C. Such high operation temperature enables the use of a wide range of fuels, varied from gas, liquid to solid. For example, methane, propane, gasoline, ethanol, and carbon have been tried as the fuels of SOFCs in literatures.[6–10]

Up to now, fuel cells are used mainly for generating electric power from chemicals, thus the fuels are typically deep oxidized to H_2O and/or CO_2 for maximizing the power generation. However, based on the reaction mechanisms, fuel cells also can be treated as the electrochemical membrane reactor, where the electrolyte functions as a membrane for separating oxygen or hydrogen in the form of ions. It is well known that many selective oxidations of hydrocarbons could also happen at the temperature range of 500–1000°C, such as the partial oxidation of methane to syngas and dehydrogenation of ethane to ethylene.[11,12] Therefore, SOFCs also could be performed as the membrane reactor for upgrading hydrocarbons to value-added products through carefully selecting the anode materials and controlling the oxygen flux. A significant advantage of fuel cells as the membrane reactor over conventional reactors is the feasibility for cogeneration of value-added chemicals and electricity. In addition, the conversion of partial enthalpy to electric power may also effectively mediate the Hotpoint problem of a catalyst under exothermic reactions.

During the past years, the application of SOFCs-type reactor for upgrading chemicals to value-added products has been tried by many groups,[13–20] and the cogeneration of electric power and syngas from methane using conventional dual-chamber SOFCs' (DC-SOFCs) reactors also has been widely investigated.[21–24] Although some progresses have been

Correspondence concerning this article should be addressed to C. Su at tuzi_ideal@163.com.

obtained, the DC-SOFCs as the reactor for cogeneration of electric power and chemicals still have some serious drawbacks. For instance, methane conversion, syngas selectivity as well as syngas production rate are all strongly affected by the polarization current, which determines the oxygen flux. Single-chamber SOFC (SC-SOFC) is a type of sealant-free fuel cell, which allows the power generation from a premixed fuel and oxidant stream in a mono chamber. Such simplified cell configuration can greatly increase the tolerance toward thermal shock, which is beneficial for electrochemical reactor application. The cogeneration of electricity and syngas from methane using SC-SOFCs was also exploited during the past years.[25,26] Very recently, we proposed that a SC-SOFC operating on a premixed CH_4-O_2 stream can realize the simultaneous high power output and syngas yield by integrating an efficient catalyst with high activity for methane partial oxidation and steam/CO_2 reforming reactions into the downstream of the SC-SOFC reactor.[26] In that study, we applied a small size disk-shape fuel cell. As we know, the methane partial oxidation is a volume expansion reaction, while the oxygen reduction over the cathode is a volume constriction reaction. Serious gas diffusion between the anode and cathode sides could appear by applying planar shape SOFCs, which could introduce strong size effect. Indeed, up to now, most good cell performances were always reported for the cells with geometric surface area of cathode less than 1 cm^2, while absolute power output larger than 1 W was seldom reported even for the SC-SOFC stack.[27–29] Instead, the gas diffusion between anode and cathode sides can be minimized by applying tubular cells due to the anode is inside and the cathode is outside of the tube.

In this study, we reported the application of flow-through tubular SOFCs for operating on CH_4-O_2 gas mixture. An attractive cell power output of about 1.5 W at the furnace temperature of 750°C was achieved after optimizing the operation conditions. A specific operation mode was further proposed, which effectively eliminated the gas interdiffusion between the anode and cathode sides, and allowed the in-situ initialization. In the end, a methane reforming catalyst was integrated into the downstream of the fuel cell to realize the cogeneration of electric power and synthesis gas from methane fuel with promising results.

Experimental

Powder synthesis

Y_2O_3 (8 mol %) stabilized zirconia (YSZ) and NiO powders were purchased from Tosoh (Japan) and Chengdu Shudu Nano-Science Co., (China), respectively. The $Sm_{0.2}Ce_{0.8}O_{1.9}$ (SDC) powder for the buffer layer was synthesized by a hydrothermal process.[30] The composite cathode materials including $Ba_{0.5}Sr_{0.5}Co_{0.8}Fe_{0.2}O_{3-\delta}$ (BSCF) and SDC powders were synthesized via a combined ethylene diamine tetraacetic acid (EDTA) - citrate acid (CA) complexing sol-gel process.[31] The $GdNi/Al_2O_3$ catalyst with the composition of 5.56 wt % Gd_2O_3, 15 wt % nickel, and 79.44 wt % Al_2O_3 was synthesized by a glycine nitrite process.[32] All the raw materials for the powder synthesis are in analytical reagent (AR) grade.

Single cell fabrication

The flow-through tubular cells applied in this study are in an anode-supported thin-film electrolyte configuration, which are composed of NiO-YSZ cermet anode (NiO:YSZ = 6:4, by weight), YSZ electrolyte, SDC buffer layer, and BSCF-SDC composite cathode (BSCF:SDC = 7:3, by weight). First, NiO and YSZ powders were mixed with polyvinyl alcohol, dextrin, and tung oil by a mini-type vacuum pugmill to make a formulation (slip) with enough plasticity for the anode substrate extrusion processing. After drying and aging at room temperature for about 1 week, the green tubular anode substrates were heated at 1100°C for 2 h in air for burning out the organics (e.g., starch and oil), which could have significant detrimental effect on the integrity of a thin-film electrolyte during the following fabrication process. A slow heating rate of 1°C min^{-1} was applied in this study for obtaining a crack-free anode substrate. A thin YSZ electrolyte layer was then deposited onto the outer surface of sintered anode by dipping the anode substrate into YSZ slurry, which prepared by the ball milling of YSZ powder in the ethanol media with solid content of about 10% in weight. The thickness of the YSZ film was controlled by the dip-coating times, generally three repeated dip-coating could result in the electrolyte thickness of around 10 μm after sintering at 1400°C. For forming the SDC buffer layer to avoid the interfacial reaction between YSZ and BSCF, the SDC suspension with solid content of about 5% was then sprayed onto the outer surface of YSZ electrolyte by using a modified spraying gun with a nozzle size of 0.35 mm (pore diameter) under the drive of 1 atm nitrogen carrier gas, and then the buffer layer was sintered at 1250°C for 5 h. Finally, the cathode layer which was prepared onto the SDC surface by the spray deposition was also attached to the SDC buffer layer surface firmly after the calcination at 1000°C for 2 h.

Characterizations

The *I-V* polarization test of the tubular SC-SOFCs was performed in a four-probe mode over a home-constructed fuel cell test workstation. Silver wires were surrounded onto both the anode and cathode to perform as the current collector to minimize the contact resistance, and the schematic diagram could been found in our previous article.[33] A Keithley 2440 digital sourcemeter was used for generating constant polarization current to the cells and also measuring the cell voltage response. For the cell in a dual-chamber mode, 3% H_2O humidified H_2 at a flow rate of 300 mL min^{-1} or 3% H_2O humidified CH_4 (300 mL min^{-1}) or CH_4-O_2 gas mixture (CH_4: 300 mL min^{-1}, O_2: 150 mL min^{-1}) as the fuel was introduced into the anode chamber, while the cathode (outer surface of the tubular cell) was exposed to ambient air. For the cell in a single chamber mode, CH_4-O_2 gas mixture (CH_4: 300 mL min^{-1}, O_2: 150 mL min^{-1}) was applied as the feed gas.

The cell microstructure was observed by environmental scanning electronic microscope (ESEM, Quanta-200), and the configuration of the tubular SOFC was performed by a digital camera (Canon 930 IS). The gas composition of the effluent gas from the fuel cell reactor was analyzed by the Varian 3800 gas chromatography. The calculation methods of CH_4 conversion, CO and H_2 selectivity, and H_2/CO ratios were given in our previous study.[32,34]

Results and Discussion

Cell morphology

Figure 1 shows the digital photos of the anode tube after sintering at 1100°C for 2 h (Figure 1a), the tubular

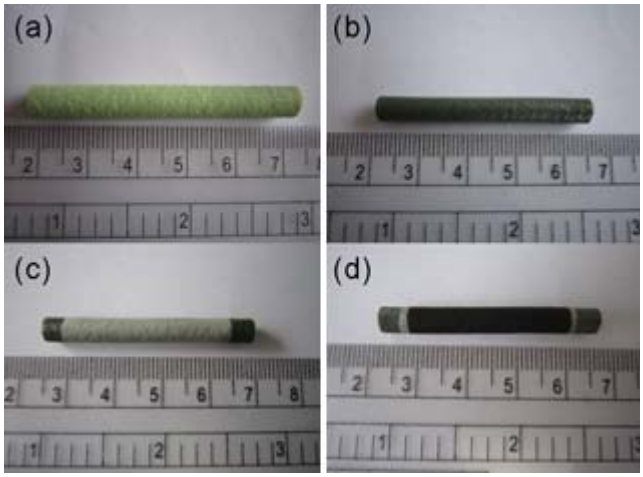

Figure 1. The digital photos of the anode tube after sintering at 1100°C for 2 h (a), the tubular anode-supported thin-film YSZ electrolyte dual-layer after sintering at 1400°C for 5 h (b), the tubular cell with the SDC buffer layer after sintering at 1250°C for 5 h (c) and the single tubular SOFC with the SDC buffer layer and the cathode layer (d).

[Color figure can be viewed in the online issue, which is available at wileyonlinelibrary.com.]

anode-supported thin-film YSZ electrolyte dual-layer after sintering at 1400°C for 5 h (Figure 1b), the tubular cell with the SDC buffer layer after sintering at 1250°C for 5 h (Figure 1c), and the single tubular SOFC with the SDC buffer layer and the cathode layer (Figure 1d), respectively. The green extruded anode tube has outer diameter of 11.0 mm and wall thickness of 1.2 mm. After the presintering at 1100°C for 2 h, the outer diameter and wall thickness of tube reduced to 10.0 and 1.1 mm, respectively. Here, the presintering process is important to create sufficient mechanical strength of the anode substrate for later dip-coating of the electrolyte layer, and to still maintain sufficient shrinkage after the sintering at 1400°C, thus ensuring the high densification of the coating electrolyte layer. The outer diameter and the wall thickness of the tube after the calcination at 1400°C decreased obviously to only 8.0 and 0.7 mm, respectively. Once the dense YSZ electrolyte layer was fabricated, no obvious further shrinkage was observed during the fabrication of SDC buffer layer sintering at 1250°C.

A typical environmental scanning electronic microscope (ESEM) image of the single tubular SOFC after the cell performance test was shown in Figure 2. The anode substrate was porous, while the cathode was more sintered as compared to anode. A relatively dense and thin cathode layer is preferred for SC-SOFCs because it can reduce the reaction rate of unwanted methane oxidation over cathode. The electrolyte layer was well densified, free of any pinholes, and had a thickness of around 15 μm. Between the cathode and electrolyte layer, a porous buffer layer was clearly observed, which had a thickness of around 3 μm. The porous nature can be explained by the relatively low sintering temperature (1250°C) and constricted sintering by the YSZ electrolyte. As it is shown, the cell components attached to each other pretty well without the observation of any delamination. The firm adhesion of the different layers in SOFCs ensures a low polarization resistance.

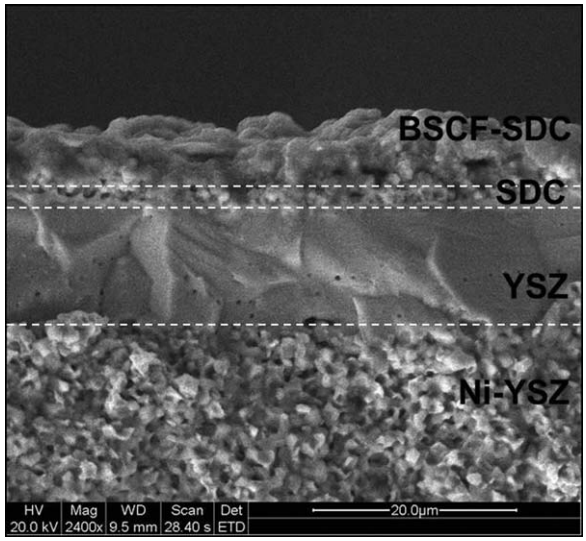

Figure 2. ESEM image of the tubular cell from the cross-sectional view.

Power generation

The as-fabricated tubular cells were first tested in dual-chamber configuration. To perform the test, both ends of the flow-through tubular SOFC were connected with flow-through quartz tubes of the similar size, as shown in Figure 3a. The fuel was fed into the anode chamber through the small quartz tube. Any local defect can cause the cell leakage and result in an obvious reduction in performance such as low open-circuit voltage (OCV) and poor power output. The typical *I-V* polarization curves of the cells operating on the three different fuels at 750°C were shown in Figure 3b. The cell showed an OCV of 1.07 V for operating on 3% H_2O humidified H_2, which is close to the theoretical value (1.11 V) based on Nernst calculation, suggesting the well densification of the electrolyte, in well agreement with the ESEM observation. When the fuel was switched to CH_4-O_2 gas mixture, the high OCV was also obtained (1.00 V), suggesting the fuel cell anode performed favorably for methane partial oxidation. As we know that the cell OCV is determined by the oxygen partial pressures at both the anode surface and cathode surface, which can be expressed by the following equation

$$OCV = \frac{RT}{4F} \ln \frac{P_{O_2}^{c}}{P_{O_2}^{a}} \tag{1}$$

where $P^{a}_{O_2}$ and $P^{c}_{O_2}$ are the oxygen partial pressure over the anode surface and cathode surface, respectively. Assuming the cathode performs ideally ($P^{c}_{O_2} = 0.21$ atm), the apparent oxygen partial pressure at the anode surface should be 4.07×10^{-21} atm based on Eq. 1. Obviously, the high activity of the nickel cermet anode for methane partial oxidation effectively consumed the oxygen in the gas mixture and lowered the oxygen potential. It also indicates that the tubular cell anode is suitable for the later operation in the single-chamber mode. The slightly lower OCVs for operating on CH_4-O_2 gas mixture than 3% H_2O humidified CH_4 fuel imply the anode performance for methane partial oxidation could be further improved by using a methane partial oxidation catalyst with higher activity to decorate the anode surface. The peak power densities (PPDs), which were determined by the OCV (U_{ocv}) and internal resistance (R_i) and

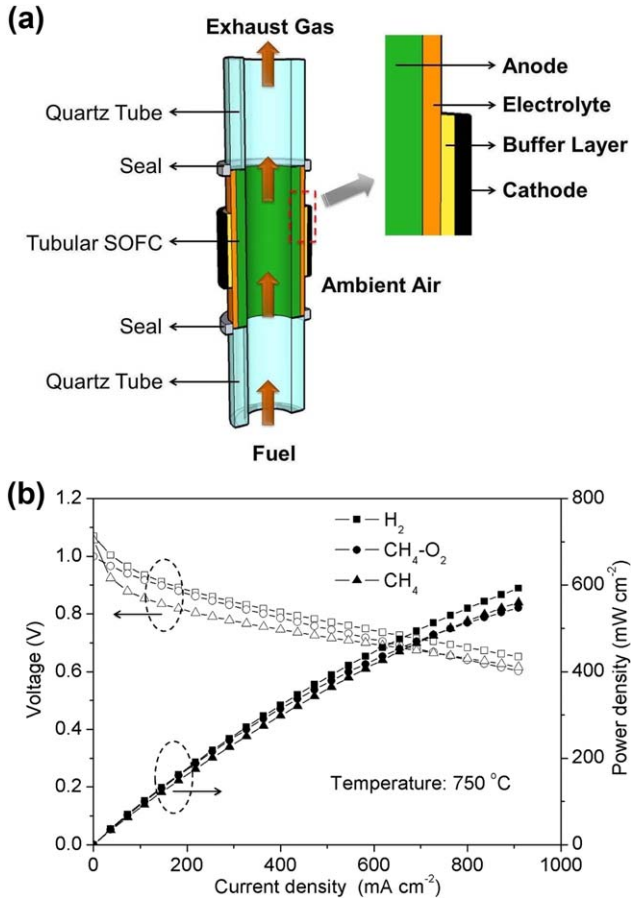

Figure 3. Schematic diagram (a) and *I-V* and *I-P* curves (b) of the tubular SOFC under dual-chamber operation at 750°C.

[Color figure can be viewed in the online issue, which is available at wileyonlinelibrary.com.]

can be calculated by the Eq. 2, achieved 521, 441, and 407 mW cm^{-2} under the current density of 926 mA cm^{-2} for the cell operating on 3% H_2O humidified H_2, 3% H_2O humidified CH_4, and CH_4-O_2 gas mixture, respectively

$$P_{peak} = \frac{U_{ocv}^2}{4R_i} \tag{2}$$

The PPDs of the cell with the effective surface area of 5.4 cm^2 have not yet achieved due to the limitation of the digital sourcemeter (Keithley 2440 with the maximum current of 5 A). According to the extrapolation, the PPDs of 723, 592, and 656 mW cm^{-2} could be obtained when the cell operated on 3% H_2O humidified H_2, 3% H_2O humidified CH_4, and CH_4-O_2 gas mixture, respectively. It signifies that the as-fabricated tubular SOFC had affordable cell performance for power generation, in particular from methane-based fuel.

The tubular SOFCs were then further tested in single-chamber configuration, and two operation modes were tried, as shown in Figure 4. In the first operation Mode A (Figure 4a), the flow-through tubular cell was directly put into a quartz socket tube with slightly larger inner diameter than the outer diameter of the tubular SOFC, and CH_4-O_2 gas mixture was introduced into the quartz tube with the gas flow direction parallel to the cell. For the second operation Mode B (Figure 4b), the tubular SOFC was mounted onto a small quartz tube, and the CH_4-O_2 gas mixture was introduced through the gap between the cathode and inner wall of the quartz socket tube, which then flowed through the tubular SOFC and, finally, exited the fuel cell reactor via the small quartz tube. As can be seen from the schematic diagram, a major difference between Modes A and B was the difference between reactors in parallel and series. It should be mentioned that, although, the sealing was also used in Mode B, the operation configuration can still be treated as the single chamber as the anode chamber and cathode chamber were open to each other and only one gas stream

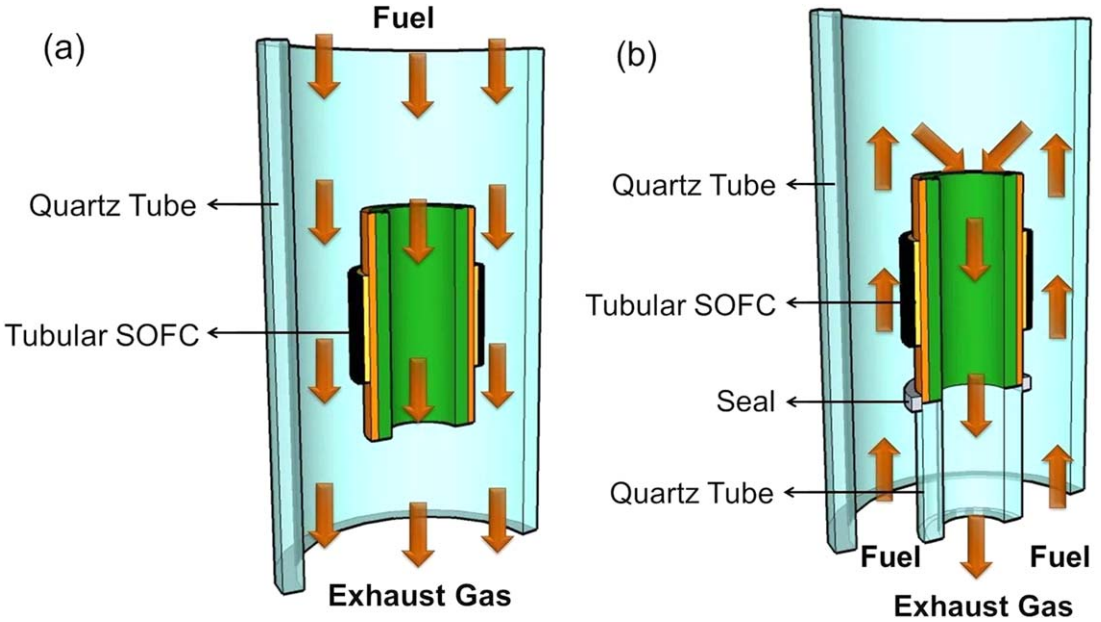

Figure 4. Schematic diagrams of the tubular SOFC under single-chamber operation Mode A (a) and Mode B (b).

[Color figure can be viewed in the online issue, which is available at wileyonlinelibrary.com.]

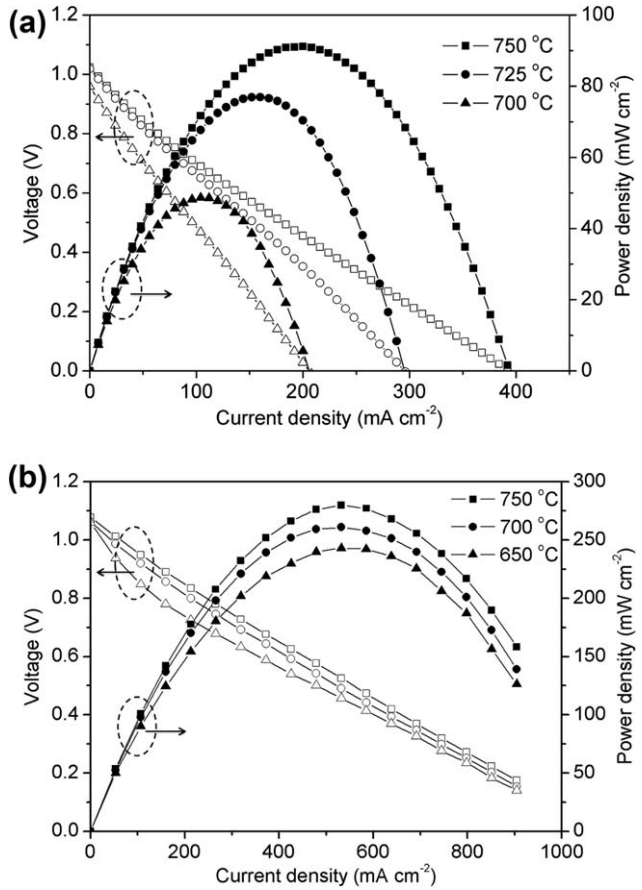

Figure 5. *I-V* and *I-P* curves of the tubular SOFC performed under single-chamber operation Mode A (a) and Mode B (b).

(CH_4-O_2) was used. In addition, the sealing in Mode B was not as strict as that in DC-SOFCs and small gas leakage was allowable.

Figure 5 shows the *I-V* polarization curves of the tubular SOFC for operating on both modes. It is important to note that the cell anode was prereduced by hydrogen before depositing the cathode layer in the cell fabrication process, and the calcination of the cathode layer was conducted in an inert gas atmosphere to avoid the reoxidation of anode. For operation Mode A, the cell showed high OCVs of 1.03, 1.02, and 0.96 V at the furnace temperatures of 750, 725, and 700°C, respectively (Figure 5a). For a fuel cell operating in single-chamber mode, its OCVs are strongly dependent on the catalytic activity and selectivity of both electrodes toward the fuel-oxidant gas mixture. If the electrodes showed no selectivity toward the gas mixture, a zero OCV should be observed. The high OCVs in this study suggest that the electrodes performed favorably toward the gas mixture under zero polarization current conditions, that is, the anode mainly functioned as a catalyst for methane partial oxidation, while the cathode was catalytically active mainly for the oxygen reduction reaction. Although in the operation Mode A, the cell showed favorable OCVs, the power outputs were relatively low with the PPDs of only 90, 76, and 48 mW cm^{-2} at the furnace temperatures of 750, 725, and 700°C, respectively. We further operated a tubular SOFC in the operation Mode B. As shown in Figure 5b, OCVs of 1.08, 1.07, and 1.06 V were reached, respectively, at 750, 700, and 650°C, which were slightly higher than those achieved by operating in the operation Mode A, suggesting the improved electrode performance in the operation Mode B, likely due to the improved gas flow configuration. The cell delivered PPDs of 279, 260, and 243 mW cm^{-2} at 750, 700, and 650°C, respectively, which were much improved as compared to those achieved via the operation Mode A. Such difference may be explained by the following reasons. In the operation Mode A, the anode and cathode were in parallel, and the inputs to the anode and cathode were the same. However, the anode only consumed fuel while the cathode only consumed oxygen. In the operation Mode B, the cathode and anode were in series. The reactant feed was first fed to the cathode where it was depleted of oxygen. The feed to the anode was then enriched in fuel. Due to greater gas concentration differences between the anode and cathode when they were operated in series, better cell power output can be achieved in operation Mode B.

To further explain the difference in the power output between two operation modes, a two-dimensional (2-D) numerical model, which was developed by one of current authors and described in more detail in Ref. 32, was applied for SC-SOFCs running on CH_4-O_2 mixture.[35] In this model, two membrane electrode assemblies of length 50 mm were placed in a gas channel in parallel to resemble a tubular SOFC for simplicity. The temperature was fixed at 750°C, and the cell load potential (E) was 0.5 V. The distribution of gas-phase species in the gas chamber is shown in Figure 6. As compared to Mode A (Figure 6a), the concentrations of H_2, CO, and CH_4 over anode are much higher in the Mode B (Figure 6b), suggesting the sufficient fuel gas was experienced, which resulted in the high cell power output in the operation Mode B. Figure 7 further presented the distribution of current density along the cell in two different operation modes. It is obvious that the current density of whole tubular cell was much higher in the operation Mode B than in the Mode A, leading to a better cell performance.

Clearly, the modestly lower power outputs than that operating in the dual-chamber configuration was originated from the nonideal behavior of the cathode. To further improve the cell performance, an optimization of the cathode composition and microstructure is needed. Anyway, a maximum power output of 1.5 W was achieved for a single cell with a cathode surface area of 5.4 cm^2 at the furnace temperature of 750°C, which is the highest value reported in the open literatures for a single SC-SOFC as far as we know.

In-situ cell initialization

Different from the DC-SOFCs, in which the fuel gas to anode chamber and oxidant gas to the cathode chamber is independent, the SC-SOFCs apply a fuel-oxidant gas mixture as the atmosphere for both the anode and cathode. It is well known that the fuel cells are usually fabricated under ambient air atmosphere, thus the nickel in the cermet anode is in the oxidation state with the form of NiO. However, sintered NiO has poor catalytic activity for methane partial oxidation, thus the initialization is an important step in the operation of SC-SOFCs. For the DC-SOFCs, the initialization is very simple, just conducting in-situ reduction with hydrogen fuel at a proper temperature as the anode and the cathode are well separated from each other. However, the initialization is much more complicated for the fuel cell operating in single-chamber mode. Applying hydrogen for the in-situ reduction of anode could also reduce the cathode as the anode and

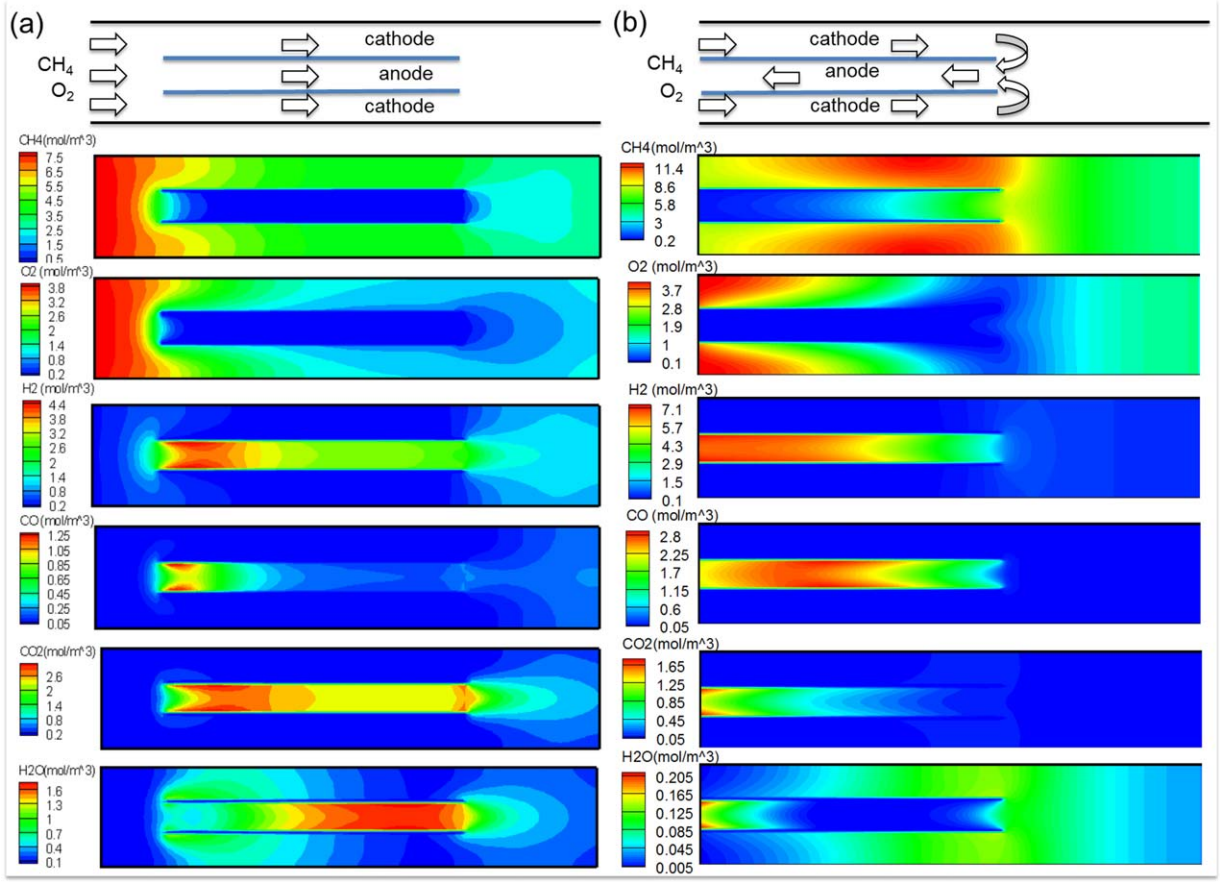

Figure 6. The 2-D distribution of gas-phase species (from top to bottom: CH_4, O_2, H_2, CO, CO_2, and H_2O in turn) in the operation Mode A (a) and Mode B (b).

[Color figure can be viewed in the online issue, which is available at wileyonlinelibrary.com.]

cathode expose to the same gas atmosphere. To initialize the SC-SOFCs, either selecting a cathode with high chemical stability against reduction, or prereducing the anode before depositing the cathode layer was typically tried. Previously, we have proposed to use a highly stable cathode material to withstand the highly reducing hydrogen during the in-situ initialization.[36] However, it is still a big challenge for us to develop a proper cathode which possesses high electrocatalytic activity for oxygen reduction, poor activity for methane oxidation as well as high chemical stability, simultaneously. Thus, the later method is more widely used in our lab. To avoid the reoxidation of anode during the calcination of fuel cell after the deposition of cathode layer, the calcination should be conducted under oxygen-free inert gas atmosphere, which increased the complexity in the cell fabrication.

In this study, an in-situ initialization of the anode becomes potentially feasible because the gas diffusion was well constricted, and the back diffusion of gas from anode to the cathode was minimized for the tubular cell in the operation Mode B. Herein, a methane partial oxidation catalyst ($GdNi/Al_2O_3$) with high activity was put inside the top part of the tubular cell, as shown in Figure 8. Once the CH_4-O_2 gas mixture passed the catalyst, the partial oxidation of methane to syngas would be induced at a proper temperature. Thus, the gas reaching the anode will be a stream of reducing syngas, instead of CH_4-O_2 gas mixture. Such reducing atmosphere could cause the reduction of nickel oxide in the anode to metallic nickel.

Figure 9 shows the operation time dependence of OCV for the cell operating on the CH_4-O_2 stream at 800°C by adopting the way as described in Figure 8. An initial value of around 0.70 V was reached, suggesting the high efficiency of the catalyst for methane partial oxidation. After operating on CH_4-O_2 stream under OCV condition for a period of around 80 min, the cell voltage increased to around 1.07 V, implying the successful initialization of the cell. We then conducted the *I-V* polarization test of the cell. As shown in Figure 10, OCVs of 1.07, 1.06, and 1.04 V were achieved, respectively, at 800, 750, and 700°C, and the corresponding PPDs reached 324, 288, and 257 mW cm^{-2}. Both the OCVs and PPDs are comparable to those obtained for the cell operating in the Mode B with the cell anode ex-situ reduced before depositing the cathode layer (Figure 5b). It suggests the anode was indeed successfully reduced, and thus greatly simplifies the fabrication process of the fuel cells, making it highly attractive for practical application. To get some information about the operational stability, a cell was polarized at a constant current density of 250 mA cm^{-2} at 700°C. As shown in Figure 11, the cell voltage was relatively stable at around 0.61 V during the test period of 600 min, indicating that the favorable cell operational stability for operating on the CH_4-O_2 gas mixture, further demonstrated its potential practical application. Anyway a much longer operation period is still required for practical application.

Electric power and synthesis gas cogeneration

Although conventional SC-SOFCs have the advantages of simpler operation mode and better thermal shock resistance as compared with DC-SOFCs, they also possess a big

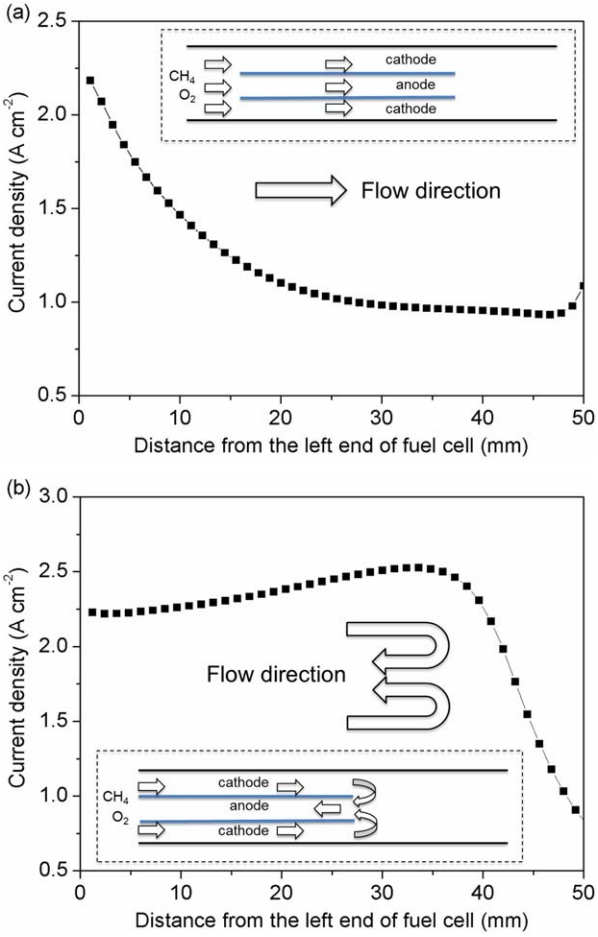

Figure 7. Distribution of local current density along the cell at the cell load potential of 0.5 V in the operation Mode A (a) and Mode B (b).

[Color figure can be viewed in the online issue, which is available at wileyonlinelibrary.com.]

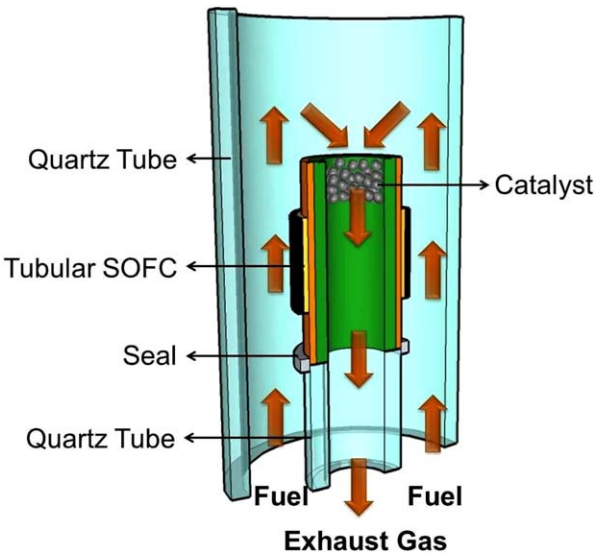

Figure 8. Schematic diagram of the tubular SC-SOFC with the GdNi/Al_2O_3 catalyst for in-situ cell initialization.

[Color figure can be viewed in the online issue, which is available at wileyonlinelibrary.com.]

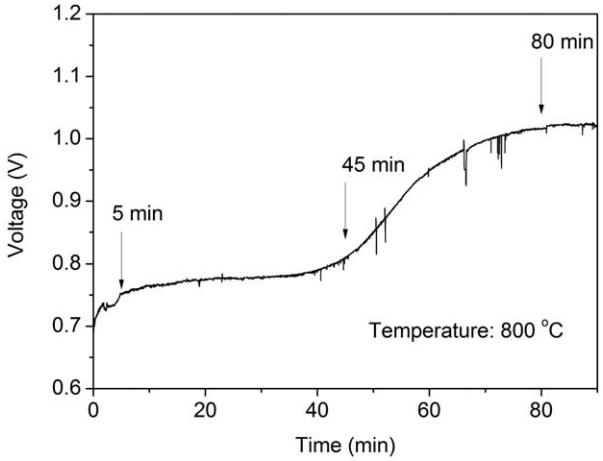

Figure 9. The time dependence of OCV for the tubular SC-SOFC with unreduced anode operating on a CH_4-O_2 gas mixture (2:1, molar ratio) at 800°C.

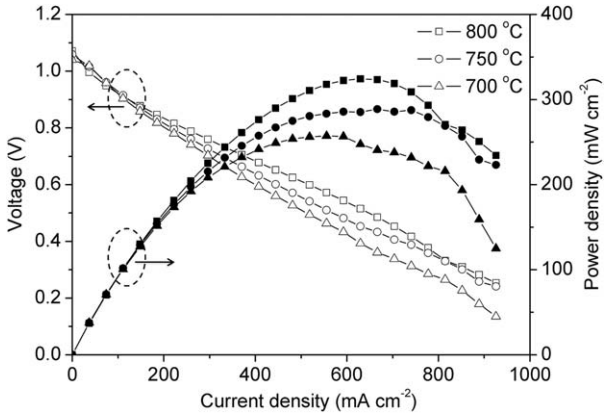

Figure 10. *I-V* and *I-P* curves of the tubular SC-SOFC after in-situ cell initialization.

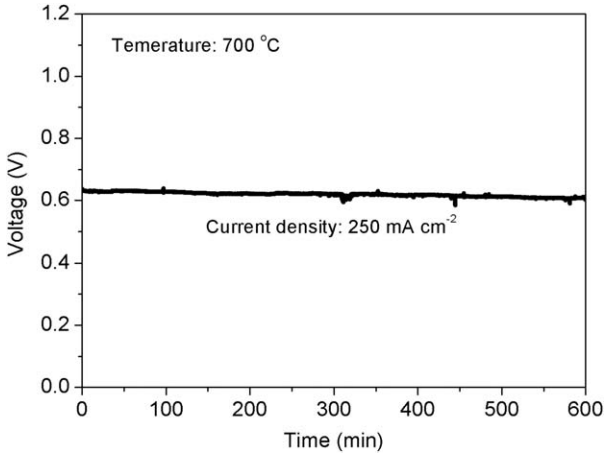

Figure 11. The performance stability of the tubular SC-SOFC after in-situ cell initialization under a constant current density of 250 mA cm^{-2} at 700°C.

drawback of low fuel efficiency. In our previous investigation about SC-SOFCs in the planar configuration, we have proposed the integration of a methane partial oxidation catalyst into the downstream of the single-chamber reactor to realize the cogeneration of electric power and synthesis gas with zero emission.[26] Similarly, a methane reforming catalyst could also be integrated into the downstream of the single-chamber tubular SOFC to allow the conversion of unreacted methane to syngas via reacting with the deep oxidation products (CO_2 and H_2O), and realize the cogeneration of electric power and synthesis gas.

To exploit the feasibility, we put the $GdNi/Al_2O_3$ catalyst on the lower end of the tubular cell as a way shown in Figure 12. The main chemical reactions occurred in the downstream were as follows

$$CH_4 + 1/2O_2 \rightarrow 2H_2 + CO$$

$$CH_4 + H_2O \rightarrow 3H_2 + CO$$

$$CH_4 + CO_2 \rightarrow 2H_2 + 2CO$$

The exhaust gas from the fuel cell reactor was, then, analyzed by the gas chromatography with the results are listed in the Table 1. To exploit the importance of the methane reforming catalyst, the exhaust gas from the tubular SOFC without the application of the catalyst was also tested. It was found that CH_4 conversion was only 49.3% even at 800°C without the application of downstream catalyst, and both CO and H_2 selectivity were low. Especially at lower temperature, CO and H_2 selectivity and CH_4 conversion was even lower. Once the downstream catalyst was applied, CH_4 conversion, CO and H_2 selectivity increased substantially to 90.6, 95.4, and 97.1%, respectively, at the same temperature. CH_4 conversion, CO and H_2 selectivity decreased with the drop of operation temperature. For example, CH_4 conversion decreased to 43.6% at 600°C. Evidently, a better methane reforming catalyst is needed at the low temperatures. As an alternative way, the methane reforming catalyst could be installed separated from the single-chamber fuel cell reactor, thus the catalyst can maintain at a proper temperature (e.g., 850°C) without the limitation by the operation of the fuel cells.

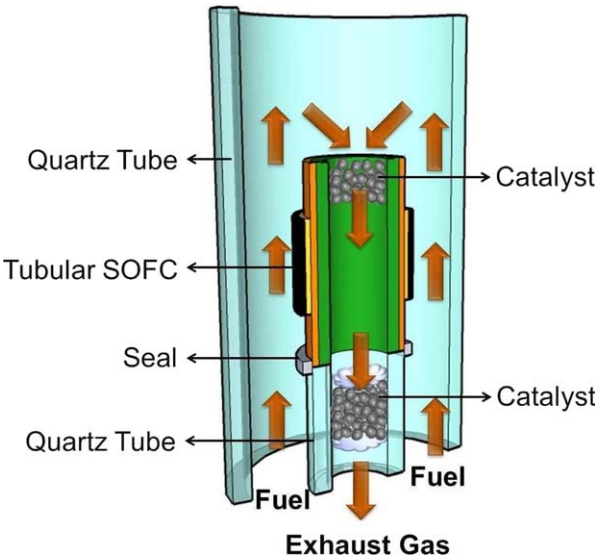

Figure 12. Schematic diagram of the tubular SOFC for electric power and synthesis gas cogeneration.

[Color figure can be viewed in the online issue, which is available at wileyonlinelibrary.com.]

Table 1. Gas Composition and H_2/CO Ratios of the Effluent Gas from the Tubular SC-SOFC Operating on CH_4-O_2 Gas Mixture with or without the Application of the $GdNi/Al_2O_3$ Catalyst

	Temperature (°C)	CH_4 Conv. (%)	CO Sel. (%)	H_2 Sel. (%)	H_2/CO ratio
With the $GdNi/Al_2O_3$ catalyst	800	90.6	95.4	97.1	2.04
	750	75.9	90.1	89.1	1.98
	700	64.6	81.6	81.8	2.00
	650	52.9	67.2	71.9	2.14
	600	43.6	50.8	59.8	2.36
Without the $GdNi/Al_2O_3$ catalyst	800	49.3	66.2	65.4	1.98
	750	44.5	55.7	59.8	2.15
	700	39.0	44.7	49.4	2.21
	650	33.4	29.4	35.6	2.42
	600	31.6	20.7	31.6	3.05

Conclusions

Small flow-through tubular SOFCs were successfully fabricated by extrusion of tubular anode substrate, dip coating of electrolyte layer and spray deposition of buffer layer and cathode layer, in combination with high-temperature sintering at proper temperatures at different fabrication stages. By controlling the operation mode of a tubular SOFC, the gas interdiffusion between the anode and cathode sides was effectively avoided, even operated in the single-chamber mode. A high OCV of 1.08 V, an attractive PPD of 300 mW cm^{-2}, and a maximum cell power output of 1.5 W for a single cell were obtained when operating on CH_4-O_2 gas mixture at the furnace temperature of 750°C. By integrating an effective and advanced catalyst into the tubular cell, in-situ initialization by CH_4-O_2 feed gas and also the cogeneration of electricity and syngas is possible.

Acknowledgments

This study was supported by National Science Research Foundation of China contract No. 51302135, China Postdoctoral Science Foundation under Grant No. 2013M531338, Science Research Foundation of Jiangsu Higher Education Institutions under Grant No. 13KJB530007, and Project of Priority Academic Program Development of Jiangsu Higher Education Institutions (PAPD). The authors acknowledge ARC Future fellowship under the contract of FT100100134.

Literature Cited

1. Steele BCH, Heinzel A. Materials for fuel-cell technologies. *Nature*. 2001;15:345–352.
2. Singhal SC. Advances in solid oxide fuel cell technology. *Solid State Ionics*. 2000;135:305–313.
3. Minh NQ. Solid oxide fuel cell technology—features and applications. *Solid State Ionics*. 2004;174:271–277.
4. Laguna-Bercero MA. Recent advances in high temperature electrolysis using solid oxide fuel cells: a review. *J Power Sources*. 2012; 203:4–16.
5. Gorte RJ. Recent developments towards commercialization of solid oxide fuel cells. *AIChE J*. 2005;51:2377–2381.
6. Laosiripojana N, Assabumrungrat S. Catalytic steam reforming of methane, methanol, and ethanol over Ni/YSZ: the possible use of

these fuels in internal reforming SOFC. *J Power Sources*. 2007;163:943–951.
7. Faro ML, Rosa DL, Nicotera I, Antonucci V, Arico AS. Electrochemical investigation of a propane-fed solid oxide fuel cell based on a composite Ni-perovskite anode catalyst. *Appl Catal B*. 2009;89:49–57.
8. Douvartzides SL, Coutelieris FA, Demin AK, Tsiakaras PE. Fuel options for solid oxide fuel cells: a thermodynamic analysis. *AIChE J*. 2003;49:248–257.
9. Huang B, Wang SR, Liu RZ, Ye XF, Nie HW, Sun XF, Wen TL. Performance of $La_{0.75}Sr_{0.25}Cr_{0.5}Mn_{0.5}O_{3-\delta}$ perovskite-structure anode material at lanthanum gallate electrolyte for IT-SOFC running on ethanol fuel. *J Power Sources*. 2007;167:39–46.
10. Adams TA II, Barton PI. High-efficiency power production from coal with carbon capture. *AIChE J*. 2010;56:3120–3136.
11. Jin RC, Chen YX, Li WZ, Cui W, Ji YY, Yu CY, Jiang Y. Mechanism for catalytic partial oxidation of methane to syngas over a Ni/Al_2O_3 catalyst. *Appl Catal A*. 2000;201:71–80.
12. Botella P, García-González E, Dejoz A, López Nieto JM, Vázquez MI, González-Calbet J. Selective oxidative dehydrogenation of ethane on MoVTeNbO mixed metal oxide catalysts. *J Catal*. 2004;225:428–438.
13. Sobyanin VA, Belyaev VD, Gal'vita VV. Syngas production from methane in an electrochemical membrane reactor. *Catal Today*. 1998;42:337–340.
14. Leal EM, Brouwer J. A thermodynamic analysis of electricity and hydrogen co-production using a solid oxide fuel cell. *J Fuel Cell Sci Technol*. 2006;3:137–143.
15. Ji BF, Wang JB, Chu WL, Yang WS, Lin LW. Acrylic acid and electric power cogeneration in an SOFC reactor. *Chem Commum*. 2009;15:2038–2040.
16. Chalakov L, Rihko-Struckmann LK, Munder B, Rau H, Sundmacher K. Reaction induced current generation by butane oxidation in high temperature electrochemical membrane reactor. *Chem Eng J*. 2007;131:15–22.
17. Wang SY, Luo JL, Sanger AR, Chuang KT. Performance of ethane/oxygen fuel cells using yttrium-doped barium cerate as electrolyte at intermediate temperatures. *J Phys Chem C*. 2007;111:5069–5074.
18. Stoukides M, Vayenas CG. Solid electrolyte aided study of the ethylene oxide oxidation on silver. *J Catal*. 1980;64:18–28.
19. Vayenas CG, Lee B, Michaels J. Kinetics, limit cycles, and mechanism of the ethylene oxidation on platinum. *J Catal*. 1980;66:36–48.
20. Vayenas CG, Farr RD. Co-generation of electric energy and nitric-oxide. *Science*. 1980;208:593–594.
21. Moon DJ, Ryu JW. Electrocatalytic reforming of carbon dioxide by methane in SOFC system. *Catal Today*. 2003;87:255–264.
22. Tagawa T, Moe KK, Ito M, Goto S. Fuel cell type reactor for chemicals-energy co-generation. *Chem Eng Sci*. 1999;54:1553–1557.
23. Huang TJ, Huang MC. Electrochemical promotion of bulk lattice-oxygen extraction for syngas generation over Ni-GDC anodes in direct-methane SOFCs. *Chem Eng J*. 2008;135:216–223.
24. Ishihara T, Yamada Y, Akbay T, Takita Y. Partial oxidation of methane over fuel cell type reactor for simultaneous generation of synthesis gas and electric power. *Chem Eng Sci*. 1999;54:1535–1540.
25. Hibino T, Iwahara H. Simplification of solid oxide fuel cell system using partial oxidation of methane. *Chem Lett*. 1993;22:1131–1134.
26. Shao ZP, Zhang CM, Wang W, Su C, Zhou W, Zhu ZH, Park HJ, Kwak C. Electric power and synthesis gas co-generation from methane with zero waste gas emission. *Angew Chem Int Ed*. 2011;50:1792–1797.
27. Wei B, Lü Z, Huang XQ, Liu ML, Jia DC, Su WH. A novel design of single-chamber SOFC micro-stack operated in methane-oxygen mixture. *Electrochem Commun*. 2009;11:347–350.
28. Akhtar N, Kendall K. Micro-tubular, solid oxide fuel cell stack operated under single-chamber conditions. *Int J Hydrogen Energy*. 2011;36:13083–13088.
29. Nagao M, Yano M, Okamoto K, Tomita A, Uchiyama Y, Uchiyama N, Hibino T. A single-chamber SOFC stack: energy recovery from engine exhaust. *Fuel Cells*. 2008;8:322–329.
30. Shi HG, Zhou W, Ran R, Shao ZP. Comparative study of doped ceria thin-film electrolytes prepared by wet powder spraying with powder synthesized via two techniques. *J Power Sources*. 2010;195:393–401.
31. Wang K, Ran R, Zhou W, Gu HX, Shao ZP, Ahn J. Properties and performance of $Ba_{0.5}Sr_{0.5}Co_{0.8}Fe_{0.2}O_{3-\delta}+Sm_{0.2}Ce_{0.8}O_{1.9}$ composite cathode. *J Power Sources*. 2008;179:60–68.
32. Wang W, Su C, Ran R, Shao ZP. A new Gd-promoted nickel catalyst for methane conversion to syngas and as an anode functional layer in a solid oxide fuel cell. *J Power Sources*. 2011;196:3855–3862.
33. Shi HG, Yang GM, Liu ZK, Zhang GR, Ran R, Shao ZP, Zhou W, Jin WQ. High performance tubular solid oxide fuel cells with BSCF cathode. *Int J Hydrogen Energy*. 2012;37:13022–13029.
34. Wang W, Su C, Ran R, Park HJ, Kwak C, Shao ZP. Physically mixed $LiLaNi-Al_2O_3$ and copper as conductive anode catalysts in a solid oxide fuel cell for methane internal reforming and partial oxidation. *Int J Hydrogen Energy*. 2011;36:5632–5643.
35. Hao Y, Goodwin DG. Numerical modeling of single-chamber SOFCs with hydrocarbon fuels. *J Electrochem Soc*. 2007;154:B207–B217.
36. Zhang CM, Zheng Y, Lin Y, Ran R, Shao ZP, Farrusseng D. A comparative study of $La_{0.8}Sr_{0.2}MnO_3$ and $La_{0.8}Sr_{0.2}Sc_{0.1}Mn_{0.9}O_3$ as cathode materials of single-chamber SOFCs operating on a methane-air mixture. *J Power Sources*. 2009;191:225–232.

Manuscript received May 21, 2013, and revision received Nov. 10, 2013.